A theory of Case II diffusion

N. L. Thomas* and A. H. Windle
Department of Metallurgy and Materials Science, Cambridge University, Pembroke Street, Cambridge CB2 3QZ, UK
(*Received* 26 *June* 1981)

A theory is proposed to explain the transport behaviour of organic penetrants in glassy polymers in terms of two basic parameters: the diffusivity of the penetrant, D, and the viscous flow rate of the glassy polymer, $1/\eta_0$. The rate controlling process for transport in these systems is considered to be diffusion of solvent down an activity gradient coupled with time-dependent mechanical deformation of the polymer glass in response to the swelling stress. The theory combines these two factors and is able to predict a wide range of observed transport phenomena from Fickian diffusion kinetics at one extreme to so-called Case II and Super-Case II behaviour at the other. The existence of a sharp front separating swollen and unpenetrated polymer is shown to result from the concentration dependence of the viscous flow rate.

Keywords Diffusion; sorption; poly(methylmethacrylate); stress; relaxation; Case II

INTRODUCTION

An important milestone in the study of anomalous diffusion phenomena (i.e. those which do not obey Fick's equations) was the recognition by Alfrey, Gurnee and Lloyd[1] of a second limiting type of behaviour. They called it Case II diffusion. It is characterized by linear kinetics and a sharp diffusion front, and it occurs in polymer–penetrant systems in which the penetrant substantially swells the polymer.

One of the earlier explanations of Case II behaviour is that due to Frisch *et al.*[2] in which an additional 'corrective' term, which is linear with time, is introduced into the Fickian-type relation for penetration depth. Their equation describes the time dependence of sorption for some systems. It does not, however, appear to be based on any clear physical principles[3], although the authors do point to the significance of the stress gradient which exists across the moving boundary. The interrelation of Fickian and Case II types of diffusion is taken a stage further by Peterlin[4,5]. He suggests that the sharp diffusion front, characteristic of the Case II process, is preceded by a region of penetrant at low concentration which forms a precursor to the front, and results from essentially Fickian controlled diffusion into the glassy material ahead of the front. In later papers[6,7] Peterlin develops his description further. He proposes that the sharp front is a consequence of a strong dependence of solubility parameter and diffusion coefficient on concentration; but he recognizes that the velocity of the front must be controlled by some independent material property, and suggests time dependent rupture and disentanglement of molecular chains as possible processes. Peterlin's formal mathematics are based on the assumption of a sharp penetrant front which moves at constant velocity. Given such a situation he is able to predict profiles both for concentration, which show a discontinuity (the sharp front), and for chemical potential, which do not. However, this treatment, because it pays no attention to the control of front velocity cannot handle situations in which the front either decelerates with time[8] or accelerates[9]. It is thus limited in scope in that it cannot predict what is probably the central aspect of Case II diffusion, that is the linear kinetics.

Similarly, Astarita and Sarti[10] demonstrate that if arbitrary assumptions are made concerning the front velocity, namely that it is zero until a critical concentration is reached and then increases according to some power of the additional concentration, then it is indeed possible to model Case II behaviour.

The fact that some process of molecular relaxation is responsible for control of the front velocity has met with growing acceptance for some time. Recent work by Sarti[11] is based on the premise that the rate controlling step at the advancing penetrant front is the formation of crazes in response to the solvent osmotic stress. Such an approach is obviously only appropriate to those systems, such as polystyrene–alkane, in which the Case II penetration of a 'solvent' is accompanied by crazing. However it is significant in that values for craze propagation rates are independently available as a function of stress for polystyrene, and that the osmotic swelling stress can be calculated for the system. Hence it is possible, albeit in terms of another equally complicated phenomenon, to understand and predict the constant rate of Case II front propagation.

The proposal that the rate controlling step at the penetrant front is the time dependent mechanical deformation of the polymer in response to the thermodynamic swelling (osmotic) stress has been made by Thomas and Windle[12], who noted the significance of the shape change imposed on the material at the front. Experimental evidence specifically supporting this deformation model has been presented more recently[13].

The work reported below, which follows from these ideas, is developed in three stages. Initially the

* Now at ICI Ltd, The Heath, Runcorn, Cheshire

0032-3861/82/040529-14$03.00

relationship between pressure, concentration and activity for a liquid swelling a polymer is considered on a thermodynamic basis alone. Next, the kinetics of swelling are calculated for an element which is thin enough to render diffusional resistance (in Fickian terms) insignificant. The rate controlling step is seen as the mechanical viscous resistance of the polymer to increase in volume and change of shape. Calculation of the kinetics demands a knowledge of the viscous response of the polymer glass which is gleaned from creep data, and also an assumption as to how this response changes as the polymer is plasticized by the penetrant. In the final state the complete diffusion process for a bulk specimen is determined by calculating change in concentration profile due to creep at constant activity, and the change in activity profile at constant activity–concentration ratio, in alternate time increments. The results are presented both as total sorption–time curves and as families of concentration profiles for a range of times.

THE RELATIONSHIP BETWEEN CONCENTRATION, PRESSURE AND ACTIVITY IN A SWOLLEN POLYMER

The thermodynamics introduced in this section are generally established and straightforward. One purpose of laying the equations out, as below, is to clarify, not only the definitions of particular terms, but also the approximations we have introduced prior to the application of the relationships in subsequent stages of the analysis.

The chemical potential per mole of diluent sorbed into a swollen polymer, with reference to a standard state is given by:[14]

$$\mu_1-\mu_1^0=RT\left\{\frac{G\bar{V}_1}{V_i}[(1-v_1)^{1/3}-(1-v_1)]+\ln v_1+(1-v_1)+\chi(1-v_1)^2\right\} \quad (1)$$

The first term in the square brackets accounts for the entropic constraint of the molecular network and the final three terms are derived from solution considerations when one component is macromolecular[15].

The symbols in equation (1) are as follows: G = molecular network parameter (number of network elements in the polymer); $\bar{V}_1$ = molecular volume of diluent; V_i = volume of unswollen polymer; v_1 = volume fraction of diluent in the swollen polymer; χ = polymer–solvent interaction parameter.

If the swelling of the polymer is opposed by an external hydrostatic pressure P which acts on the polymer but *not* on the surrounding liquid, then the sorption of one mole of diluent of volume $\bar{V}_1N_A$ will cause external work $P\bar{V}_1N_A$ to be done (N_A is Avogadro's number), so that equation (1) becomes:

$$\mu_1-\mu_1^0=P\bar{V}_1N_A+RT\left\{\frac{G\bar{V}_1}{V_i}[(1-v_1)^{1/3}-(1-v_1]+\ln v_1+(1-v_1)+\chi(1-v_1)^2\right\} \quad (2)$$

The same equation is applicable if the opposition to swelling, additional to that accounted for in entropic terms, comes, not from external pressure but from kinetic immobility of the molecular network. It can thus be applied to the swelling of a glass. The pressure P can be considered as an additional pressure in the imbibed liquid which affects the chemical potential and points to the relevance of the osmotic analogy.

In introducing activity, a_1, we take its more traditional definition as:

$$\mu_1-\mu_1^0=RT\ln a_1 \quad (3)$$

where μ_1^0 is the chemical potential at standard temperature and pressure. This means that the activity will depend on pressure as well as concentration. In some situations this is seen as a disadvantage, where activity is needed as a measure of departure from ideality alone, and the pressure sensitivity is removed by redefining the standard chemical potential μ_+^0, as:

$$\mu_+^0=\mu_1^0+V_i(P_+-P_0)$$

In the analysis which follows non-ideality is not of significant importance; whereas activity, as a measure of thermodynamic potential in conditions of varying concentration and pressure, is preferable to chemical potential which becomes negative without bound as concentration is reduced. (This is in fact the reason why G. N. Lewis introduced activity in the first place.) We thus use activity in its pressure dependent form as defined by equation (3). Combination of equations (2) and (3) gives the relationship between activity of the penetrant, its volume fraction and the additional pressure P:

$$\ln a_1=\frac{P\bar{V}_1N_A}{RT}+\frac{G\bar{V}_1}{V_i}[(1-v_1)^{1/3}-(1-v_1)]+\ln v_1+(1-v_1)+\chi(1-v_1)^2 \quad (4)$$

For equilibrium conditions where the swollen polymer is immersed in pure penetrant liquid of unit activity, then $a_1=1$ and the right-hand side of equation (4) will be zero.

The behaviour of this equation has been explored by substituting values for $\bar{V}_1$ and χ for the system PMMA–methanol, i.e. $\bar{V}_1=6.72\times10^{-29}$ m^3 and $\chi=1.0$ at 24°C where the equilibrium swelling gives $v_1=0.275$[8]. Hence for $a_1=1$ and $P=0$ it is possible to calculate $G\bar{V}_1/V_i$. It is 0.233.

Figure 1a is a plot showing the relationship between pressure and concentration for a range of activities.

At this point we introduce the volume ratio $\bar{v}$ which is the ratio of volume fraction of penetrant, v_1, to the equilibrium volume fraction under conditions of zero extra pressure and unit activity. It is useful, because on imposing the approximation that the chemical behaviour is 'ideal' we can write:

$$\bar{v}=(a_1)_{P=0}$$

Hence from equation (4)

$$\ln\bar{v}=\frac{G\bar{V}_1}{V_i}[(1-v_1)^{1/3}-(1-v_1)]+\ln v_1+(1-v_1)+\chi(1-v_1)^2$$

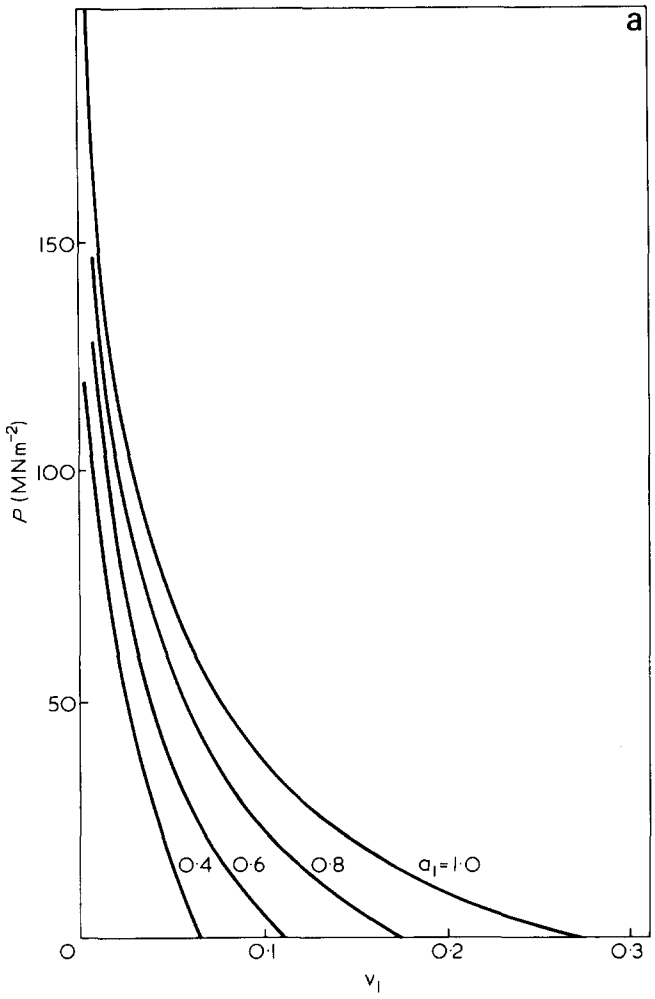

Figure 1a Relationship between pressure, P, and volume fraction of solvent in the swollen polymer, v_1 for a range of activities, as determined from equation (4)

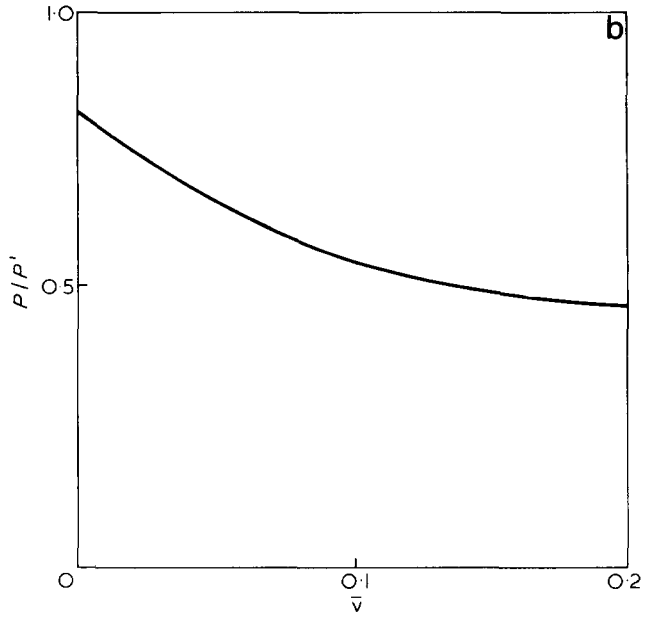

Figure 1b Comparison of the pressure–volume fraction ($P - v_1$ and $P' - v_1$) relationships at unit activity as calculated from equations (4) and (5), where equation (5) is a simplified form of equation (4), and is applicable to ideal situations. The ratio P/P' lies between 0.8 and 0.5, and represents the uncertainty associated with the use of the simplified equation as used in the development below

and thus:

$$P = \frac{RT}{\bar{V}_1 N_A} \ln\left\{\frac{a_1}{\bar{v}}\right\} \tag{5}$$

which is one simple form of the osmotic pressure equation, and is identically true for ideal solutions.

The effect of the assumption of chemical ideality on the pressure–concentration–activity relationship for the PMMA–methanol system is shown in *Figure 1b* for an activity of unity. P is the pressure calculated according to equation (4) and P' that using the approximate equation (5).

RESPONSE OF GLASSY NETWORKS TO SWELLING PRESSURE

The fact that a glassy network offers resistance to expansion at finite strain rates which is over and above its entropic resistance, means that additional pressure develops in the swelling liquid. The swelling kinetics will depend on the viscous response of the network to this internal pressure. It is necessary to know this, but as hydrostatic creep tests on glassy polymers are difficult, particularly in tension, direct data are not available. Substantial volume expansion of a glass will involve both the pulling out of loops of molecular segments and the reorientation of these segments, in fact the same mechanisms as those involved in simple elongation. We therefore make the assumption that the viscosity component controlling the retarded elasticity of the network is the same for volume expansion as it is for elongation. Additionally the fact that the volumetric expansion in Case II diffusion is, *per se*, associated with a change in shape, would appear further to validate the assumption.

THE SWELLING KINETICS OF A VERY THIN ELEMENT OF THE GLASSY POLYMER

In considering a very thin element of polymer we dismiss any diffusional resistance from the kinetic treatment. We assume therefore that the instant the thin element is immersed in the penetrant liquid the penetrant achieves unit activity throughout the element. Furthermore, in order to relate the process as closely as possible to Case II transport the element is envisaged as being bonded to a rigid inert substrate so that it cannot increase in volume without at the same time changing in shape (*Figure 2*).

Before the swelling response of the element can be calculated it is helpful to make two further assumptions:

(i) The increase in volume on swelling is taken as being proportional to the volume of penetrant absorbed. This

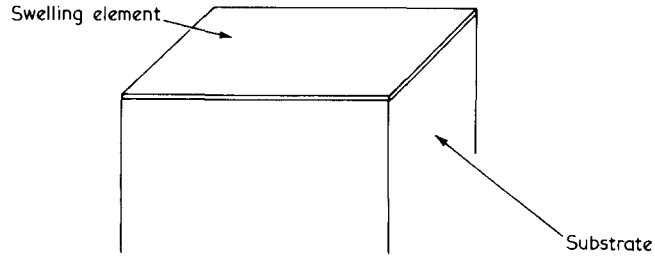

Figure 2 Schematic diagram illustrating the concept of a very thin element of polymer which is prevented from increasing in area on swelling by its attachment to a rigid inert substrate

assumption has been used by other authors[3,16] and shown to be reasonable for the PMMA–methanol system[8,17].

(ii) The viscosity of the polymer decreases exponentially with increasing penetrant concentration according to:

$$\eta = \eta_0 \exp[-M\bar{v}] \tag{6}$$

where M is a constant, η_0 the viscosity of the unswollen polymer. We use the simplified equation for swelling pressure (equation (5)) which for the condition of unit activity (reasonable when considering a very thin sheet element), becomes:

$$P = \frac{RT}{\bar{V}_1 N_A} \ln\left\{\frac{1}{\bar{v}}\right\} \tag{7}$$

The response of the element to the pressure is expressed as a strain rate, and in view of the uncertainties discussed in the previous section as to whether the resistance either to volumetric expansion or to shape change is the rate controlling step, we choose the simple viscosity relationship that:

$$\frac{d\varepsilon}{dt} = \frac{P}{\eta} \tag{8}$$

Because of the unidirectional nature of Case II swelling the deviatoric strain is directly related to the increase in volume, and if we define k as $\varepsilon/\bar{v}$ then:

$$\frac{d\bar{v}}{dt} = \frac{P}{\eta k} \tag{9}$$

Substitution of equation (7) for P and equation (6) for η into equation (9) gives:

$$\frac{d\bar{v}}{dt} = \frac{-RT}{\bar{V}_1 N_A k \eta_0} \ln(\bar{v}) \exp[M\bar{v}] \tag{10}$$

Numerical integration of this equation will give the fractional swelling of the very thin sheet element as a function of time. However, before this exercise is carried out it is of course necessary to give values to the various parameters.

ESTIMATION OF PARAMETERS OF EQUATION (10) FOR THE SYSTEM PMMA–METHANOL

Working in terms of the system PMMA–methanol at 24°C, the value of the product $\bar{V}_1 N_A$ can be readily found. It is taken as 40.5×10^{-6} m^3. From experimental data[12], k, the ratio $\varepsilon/\bar{v}$, is measured as 0.23. Values for the viscosity of PMMA glass at 24°C, η_0, and the exponential factor M are not as readily accessible. The value of η_0, as determined from creep tests, depends on applied stress as well as temperature. For example creep data at 20°C[18] apparently yield viscosities of 10^{17}, 3×10^{15} and 3×10^{14} N s m^{-2} at stresses of 10, 20 and 30 MN m^{-2} respectively. In an attempt to obtain further values of viscosity for comparison we have used various 20°C data[19] and substituted the strains at different times into the equation for creep strain derived from a standard linear solid. Taking the elastic moduli to be 1 GN m^{-2} for the glass component and 10 MN m^{-2} for the rubber, the viscosity of the dashpot element of the model was 3×10^{14} N s m^{-2} for a stress of 15 MN m^{-2}, and 8×10^{13} N s m at 45 MN m^{-2}. On an order of magnitude scale the agreement is reasonable with the data of Turner[18] and we have chosen a value of $\eta_0 = 2 \times 10^{14}$ N s m^{-2} to represent the viscosity of PMMA glass under conditions of Case II diffusion at 24°C.

The value of M is the coefficient of the exponent in equation (6) which describes the effect of concentration of the sorbed species on viscosity. It is not easy to determine independently of a diffusion experiment. We have attempted to estimate a reasonable value on the basis of observations of the shape relaxation behaviour of swollen specimens at the point at which the sharp (Case II) fronts meet in the centre of the specimen. The effect has been fully documented in a previous paper[17], but the information relevant to this issue is that at 24°C the initial shape relaxation rate of equilibrium swollen PMMA at a distortion strain of around 10% is about 4%/hour or 1.2×10^{-5} s^{-1}. Again on the basis of a rubber modulus of 10 MN m^{-2} the internal distortion stress acting on the polymer in the initial stages of shape recovery is of the order of 1 MN m^{-2}. Creep data on unswollen polymer at such low stresses do not seem to be available; however, the data of ref 19 cover a wide range of stresses from 3.5 MN m^{-2} upwards, and extrapolation indicates an initial strain rate of 3×10^{-11} s^{-1} for a stress of 1 MN m^{-2}. Thus for $\bar{v} = 1.0$ (i.e. equilibrium swelling at 24°C), and using equation (6) we have:

$$\frac{\dot{\varepsilon}_{\text{unswollen}}}{\dot{\varepsilon}_{\text{swollen}}} = \frac{3 \times 10^{-11}}{1.2 \times 10^{-5}} = \frac{\eta}{\eta_0} = \exp[-M]$$

Thus $M \simeq 13$.

These choices for the fixable parameters lead to a value of 1.35×10^{-6} m^3 s^{-1} for the pre-ln factor in equation (10), and although they are physically the most reasonable, the sensitivity of the model predictions to changes in η_0, M and the diffusivity D is examined below.

CALCULATED SWELLING KINETICS FOR A THIN ELEMENT OF PMMA IN ETHANOL

Figure 3 shows the results of numerical integration of equation (10) for a number of values of the exponential factor, M, which span the suggested value of 13. The autocatalytic nature of the process is apparent, the element taking up solvent only slowly at first but this rate rapidly accelerating towards equilibrium sorption.

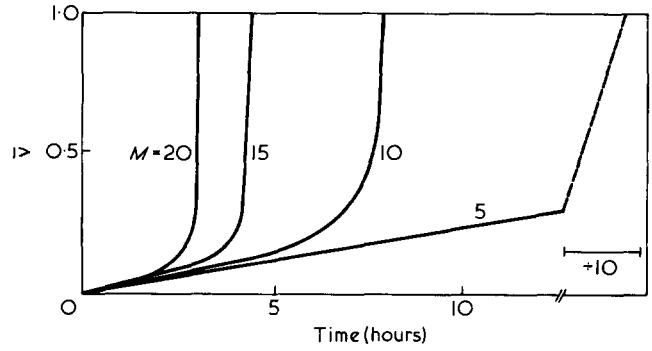

Figure 3 Curves calculated using equation (10), showing the sorption kinetics for the penetration of methanol into a thin constrained element of PMMA at 24°C. Curves are drawn for different values of M, which is most likely to lie between 10 and 15

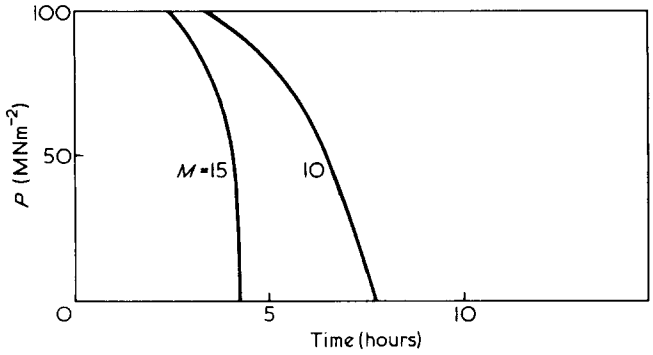

Figure 4 The variation in pressure in the PMMA element with time for *M* values of 10 and 15. The pressure remains high until rapid swelling commences at the end of the induction period

Figure 4 is a pressure-time relationship for two values of M, obtained by combining equation (7) with the data from *Figure 3*. The absolute values are surprisingly high, and approach and indeed exceed the accepted yield stress of PMMA at low solvent concentrations.

THE APPROACH TO CALCULATING CASE II KINETICS

The rate of swelling for a surface element in which the penetrant activity is constant and unity is given by equation (10) and numerical integration generates the concentration–time curves of *Figure 3*. In the case of a bulk specimen however, thin elements parallel to, but remote from, the surface will be swelling under conditions of reduced penetrant activity. The activity will gradually increase with time as determined by the diffusional resistance of the material separating the element from the surface. We are therefore faced with three operations: the modification of equation (10) to handle an element remote from the surface by including an activity term which increases with time, the calculation of the activity in the sample as a function of time and position, and the combination of these varying parameters so as to give the concentration of penetrant as a function of both time and position.

The first operation is simple, equation (10) becomes for element i experiencing penetrant activity a:

$$\left\{\frac{d\bar{v}}{dt}\right\}_i = \frac{-RT}{\bar{V}_1 N_A k \eta_0} \ln\left\{\frac{\bar{v}}{a}\right\}_i \exp[-M\bar{v}] \qquad (11)$$

(a is equivalent to a_1 of equations (3)–(5). The subscript 1 has been dropped to make way for i indicating the element under consideration.) The rate of change of the activity in an element i is obtained from the restatement of Fick's first equation in terms of chemical potential as suggested by Gibbs[20] and subsequently used by Park[21]; it is:

$$J = -D^* \frac{\bar{v}}{a} \cdot \frac{da}{dx} \qquad (12)$$

where J is the flux and D^* the thermodynamic diffusion coefficient.

Hence the change of concentration in a thin element of unit thickness in time interval Δt is given by the difference between the fluxes in and out across the planar boundaries; thus

$$\left\{\frac{\Delta\bar{v}}{\Delta t}\right\}_i = J_1 - J_2 = D_2^* \left\{\frac{\bar{v}}{a}\right\}_2 \cdot \left\{\frac{da}{dx}\right\}_2 - D_1^* \left\{\frac{\bar{v}}{a}\right\}_1 \cdot \left\{\frac{da}{dx}\right\} \qquad (13)$$

and

$$\left\{\frac{\Delta a}{\Delta t}\right\}_i = \left\{\frac{\Delta a}{\Delta \bar{v}}\right\}_i \cdot \left\{\frac{\Delta \bar{v}}{\Delta t}\right\}_i$$

As the integration of equation (13) will be carried out over finite elements of x and t, it is best expressed in terms of the values of a, $\bar{v}$ and D^* at three successive elements $i-1$, i, $i+1$, as follows:

$$\left\{\frac{\Delta a}{\Delta t}\right\}_i = \left\{\frac{\Delta a}{\Delta \bar{v}}\right\}_i \left[\left\{\frac{D^*_{i+1} + D^*_i}{2}\right\} \cdot \left\{\frac{\bar{v}_i + \bar{v}_{i+1}}{a_i + a_{i+1}}\right\} \cdot (a_{i+1} - a_i) - \left\{\frac{D^*_{i-1} + D^*_i}{2}\right\} \cdot \left\{\frac{\bar{v}_i + \bar{v}_{i-1}}{a_i + a_{i-1}}\right\} \cdot (a_i - a_{i-1})\right] \qquad (14)$$

The combination of equations (11) and (14) is based on the fact that for each time increment the change

$$\left\{\frac{\Delta\bar{v}}{\Delta t}\right\}_i$$

is calculated by equation (11) at constant activity, and thus directly related to

$$\left\{\frac{\Delta\bar{v}/a}{\Delta t}\right\}_i$$

and the change

$$\left\{\frac{\Delta a_i}{\Delta t}\right\}_i$$

is calculated at constant $(\bar{v}/a)$ ratios.

The constancy of $(\bar{v}/a)$ during a given 'diffusion' movement means that the first item of the RHS of equation (14) is in effect $(a/\bar{v})_i$. The calculation thus proceeds by first determining the change in activity profile in a small time interval for a fixed profile of $\bar{v}/a$, and then, using the modified activity profile, determining the change in the $\bar{v}/a$ profile. The new $\bar{v}/a$ profile is then used to calculate another activity profile, and so on. The logic of the method can perhaps be better seen by looking at it in a slightly different way. For a given element and time increment, the creep process controls $\Delta\bar{v}$ according to equation (11). The activity is then adjusted so that $\Delta\bar{v}$ which will result from diffusion and is given by equation (13), converges to the value 'permitted' by equation (11). The next creep controlled increment, $\Delta\bar{v}$, is then determined using the updated values of $\bar{v}$ and a. The concentration profiles are not significantly affected if for each cycle, the $\Delta a/\Delta\bar{v}$ term of equation is set using the increment values of the preceding cycle rather than the prevailing $a/\bar{v}$ value. On average, the complete transport sequence is completed in about 20 000 time steps, where the full thickness of the specimen is divided into 50 elements. Trial runs using shorter time intervals produced identical results. The procedure was initialized by setting

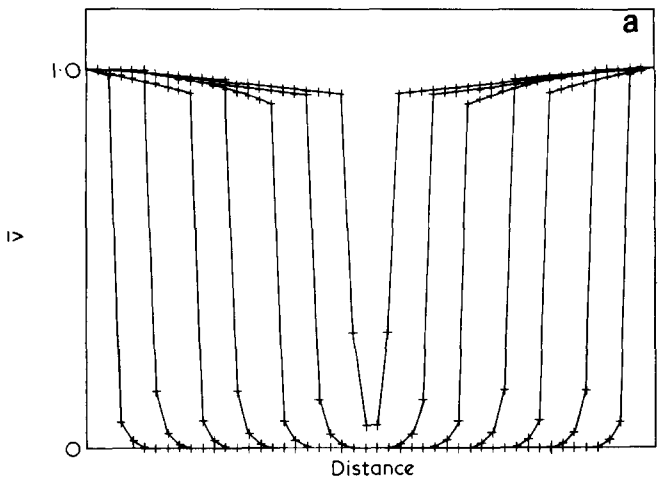

Figure 5a Diagram showing the concentration profiles calculated at 10 h intervals for a 1 mm thick specimen showing typical Case II behaviour. The parameters used for this calculation are appropriate to the system PMMA–methanol at 24°C. The diffusivity, D, is 10^{-14} m^2 s^{-1}. The viscous flow (creep) rate of the unpenetrated polymer ($1/\eta_0$) is 5×10^{-15} s^{-1} (MN m^{-2})$^{-1}$ and the factor M is 15

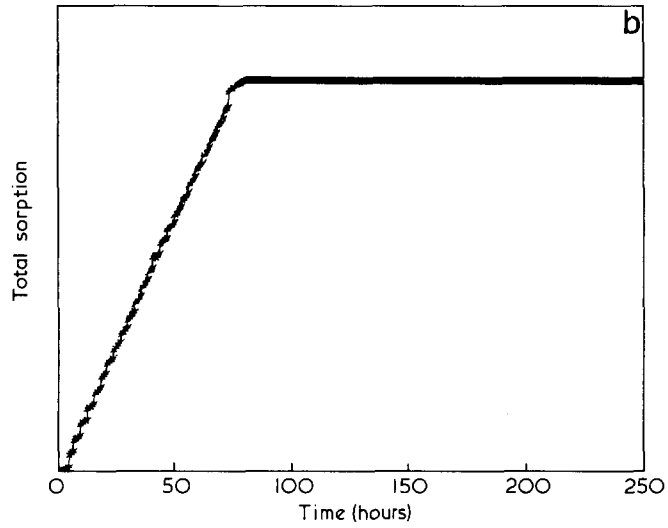

Figure 5b Total sorption plot corresponding to the profiles of *Figure 5a*

$(a)_{n=1} = 1$, $(a)_{n\neq 1} = 10^{-5}$ and $(\bar{v})_n = 10^{-5}$. The choice of 10^{-5} instead of zero being made to facilitate the computing.

CHOICE OF A VALUE FOR THE DIFFUSION COEFFICIENT, D

The literature on diffusion in glassy polymer–penetrant systems quotes a considerable range of values for D (for example, ref 22) which in any case are dependent on the thermal history of the glass. For the purposes of calculating the transport kinetics we have selected a value of 10^{-14} for D at 24°C, and have assumed that it increases exponentially with methanol concentration to reach a value of 5×10^{-12} for equilibrium sorption where the polymer has become, all but, a rubber. These values are chosen as being both typical and reasonable; however, considerable uncertainty must remain. In fact, the level of uncertainty which we are accepting means that it is not worth while to correct for increasing thickness of the specimen as the swelling proceeds, which would amount to a modification in D of around 25% only.

CALCULATION OF TRANSPORT KINETICS AT 24°C

By combination of equations (11) and (14) as already described, activity and concentration have been calculated as a function of both time and position for a sheet sample. Successive time cycles generated developing concentration profiles, from which additional parameters such as total sorption as a function of time have been derived. The constants used were those already discussed with the exception of the exponential factor M which has been 'rounded up' from 13 to 15.

Figure 5a shows the calculated developing concentration fronts for a 1 mm thick PMMA specimen at 24°C. The profiles are drawn at time intervals of 10 h. The first significant fact is that the advancing fronts are sharp to within the resolution of the calculation, that is (20 μm). They move at a constant rate and there is a small concentration gradient behind them. There is also evidence for a small 'Fickian' precursor ahead of the fronts. The apparent fluctuation in the concentration gradients behind the fronts does not represent any instability in the calculation, but is due to the finite distance increments used. Using smaller distance increments reduces the scatter at the expense of increased computer time.

Figure 5b is a plot of the total sorption against time. The uniform penetration of the step profiles apparent in *Figure 5a* produces the linear increase in sorption (usually measured as weight increases) with time. The penetration is completed after 78 h.

Considering the difficulty in the exact assessment of parameters such as D, η_0 and M, the fact that calculated kinetics are those typical of Case II is encouraging. However, the level of agreement of total sorption time with that measured at 24°C (91 h, *Figure 6b*) for a 1.18 mm thick sample must be fortuitous. The experimental profile at 60 hours determined using the iodine tracer method[8] drawn in *Figure 6a* does not show a clear diffusion gradient behind the fronts (although this becomes much more apparent in 3 mm thick specimens[8]). It also gives no indication of precursors ahead of the fronts but this may be because the tracer method is unreliable at low penetrant concentrations. The realism of the calculated kinetics appears to suggest that the theory is meaningful; furthermore, closer examination of the calculated sorption curve suggests that a small induction period of about five hours is predicted. Such an induction period has been noted before on several occasions[13,23–25] (and is indeed just apparent in the experimental data of *Figure 6b*). It has hitherto, if anything, been explained in terms of a non-typical surface effect. The small induction period in the calculated sorption curve seems to imply that such a period is a fundamental characteristic of Case II sorption.

PROFILES FOR ACTIVITY AND PRESSURE

As a direct consequence of the method of calculation of the concentration profiles developed above, the activity profiles are also available, and the pressure profile may be readily worked out using equation (5). *Figure 7* is a plot of activity, concentration and pressure profiles in the region of the front, corresponding to *Figure 5a* at a time of 40 h. The activity profile does not show a sharp step, although because of the influence of the concentration profile through $D(\bar{v})$, it is not typically 'Fickian'. The region immediately ahead of the sharp concentration front, in

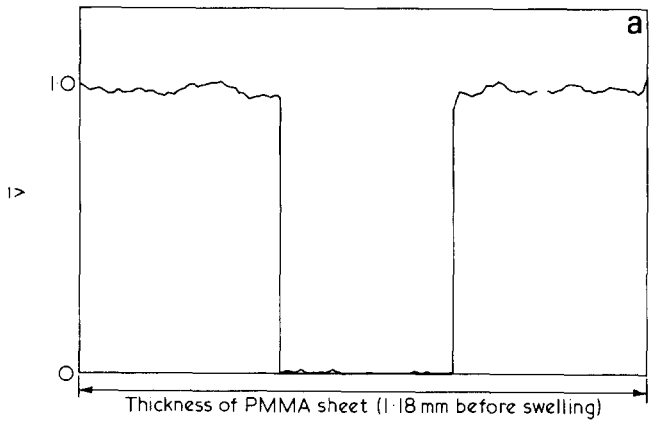

Figure 6a Experimental profile of methanol in a 1 mm thick PMMA sheet after 60 h at 24°C

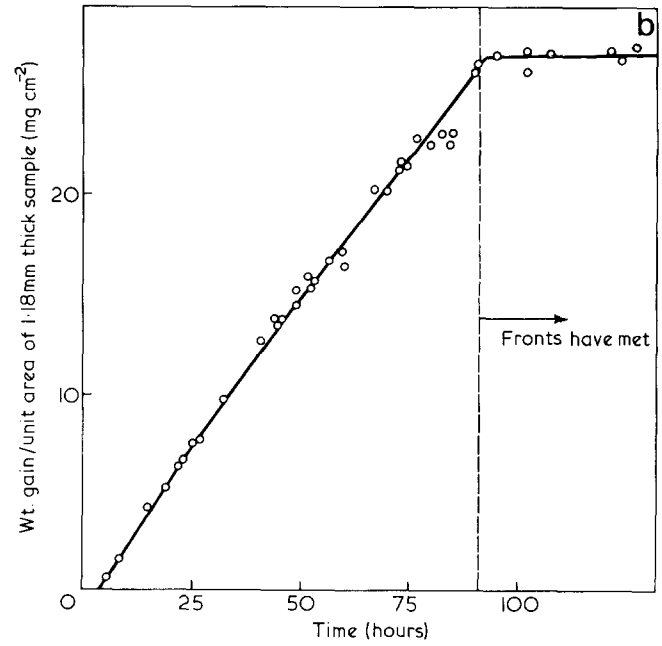

Figure 6b Experimental sorption plot for methanol in 1 mm thick PMMA at 24°C

which the activity is much greater than the concentration, is the region in which the small amount of sorbed liquid is under comparatively high pressure. The values of pressure are those which are being resisted by the molecular network, and which relax as the polymer glass deforms. At the front itself, rapid transport of the sorbed species down the concentration step is opposed by an equally steep pressure gradient in the opposite direction. Just as the iodine doping does not reveal the concentration precursor, there has, as yet, been no reported observation of phenomena which can be linked directly to this pressure profile. The constraint effect of the glass, however, might be expected to lead to some measure of deviatoric elastic strain which should be observable as birefringence.

PROFILES FOR CONCENTRATION INDEPENDENT DIFFUSIVITY

One argument against deformation control as the basic process of Case II diffusion, is that step-like profiles can result from a discontinuity in the diffusivity–concentration relationship such as might occur at T_g. Sharp profiles can indeed be generated where there is a D–C discontinuity[26]; however, not only is there doubt whether such a discontinuity occurs at T_g, for both D and C increase very rapidly in this temperature range, but it has been shown recently[13], that Case II diffusion can occur at low temperatures where the swollen phase is still a glass.

Notwithstanding this debate, it is important to check that the sharp fronts predicted in our calculations are not in any way dependent on the concentration dependence of D. Accordingly, we calculated profiles where the diffusivity was held constant at a value of roughly midway between the unswollen and fully swollen limits. *Figure 8* is

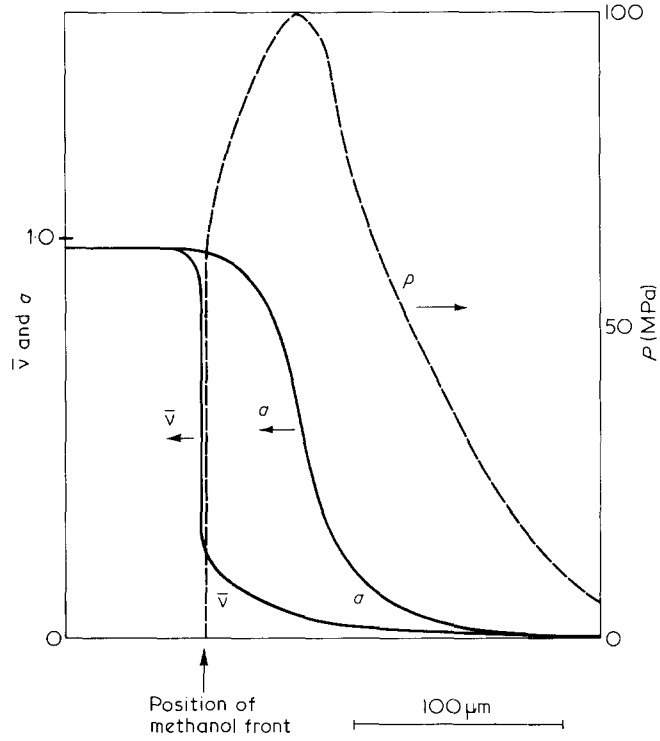

Figure 7 Calculated fractional concentration ($\bar{v}$), activity (a) and pressure (P) profiles in the region of the penetrant front after 40 h, for methanol in PMMA at 24°C. The horizontal scale is expanded in comparison with the previous profile plots and the left hand limit of the diagram does not correspond to the specimen surface

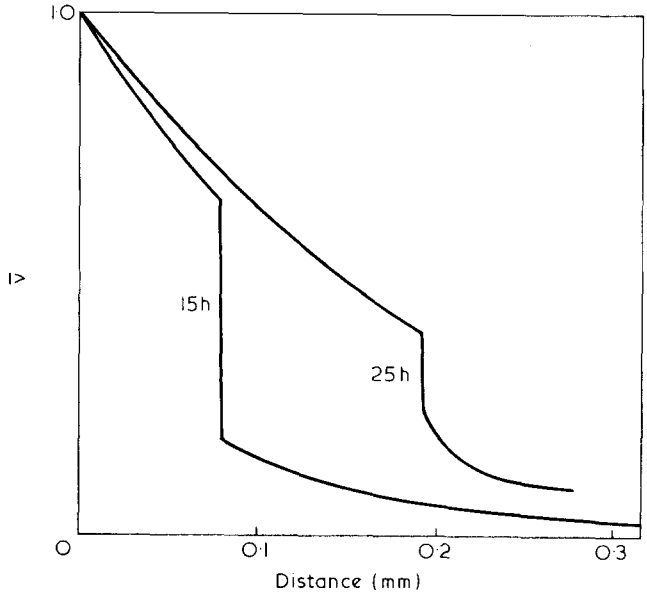

Figure 8 Penetrant concentration profiles at 15 h and 25 h calculated under the same conditions as those in *Figure 5a* except that the diffusivity is held independent of penetrant concentration at a value of $D = 8 \times 10^{-13}$ m^2 s^{-1}

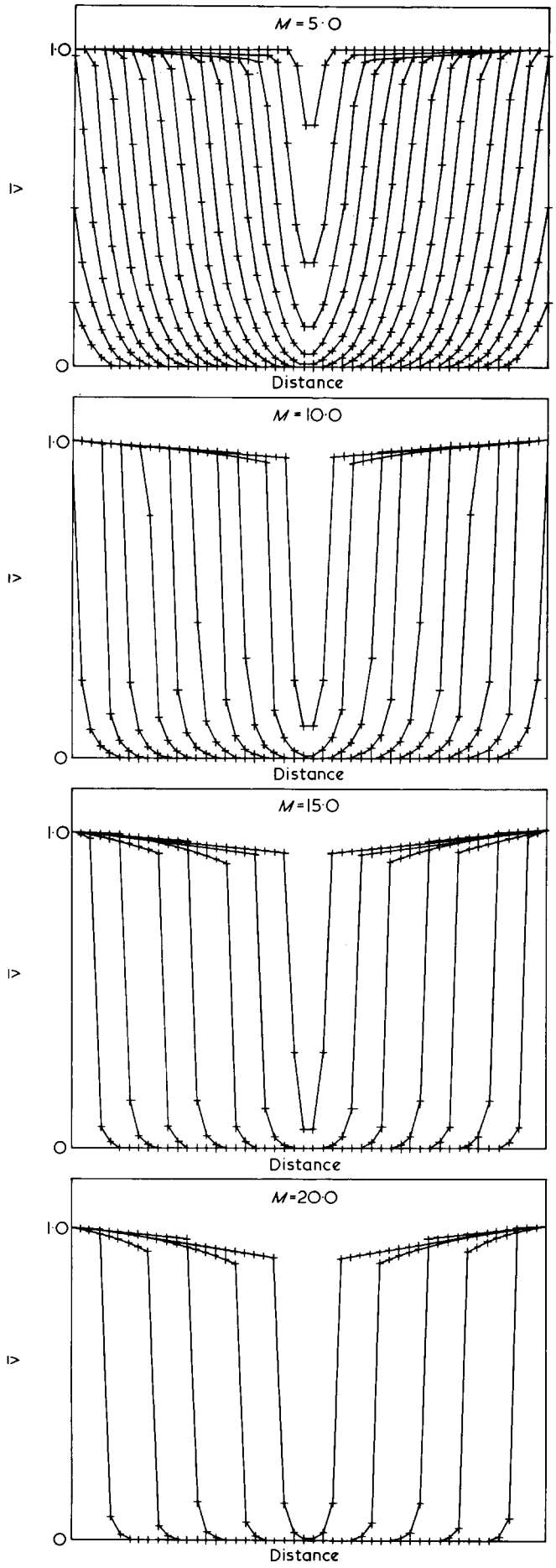

Figure 9 Effect of varying M on the calculated Case II profiles. As before, the diffusivity, D, is set at 10^{-14} m^2 s^{-1} and the viscous flow rate ($1/\eta_0$) at 5×10^{-15} s^{-1} (MN m^{-2})$^{-1}$. The plot for M = 15 is the same as *Figure 5a*

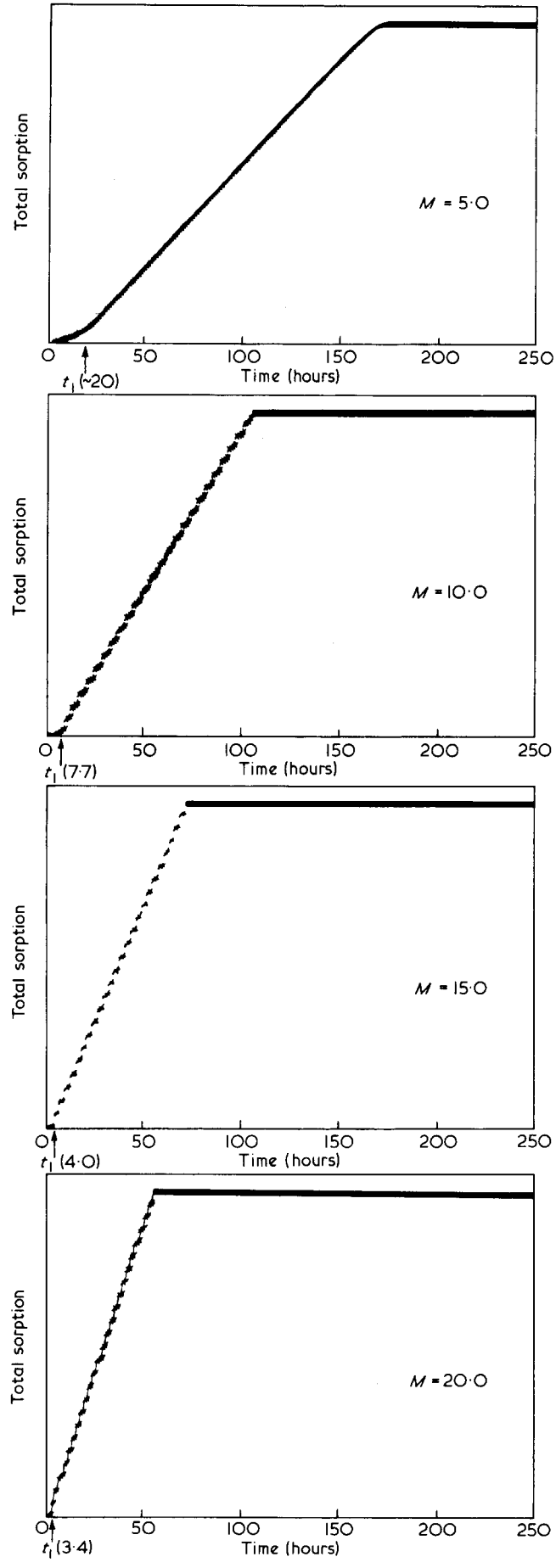

Figure 10 The effect of varying M on the sorption plots corresponding to the profiles of *Figure 9*. The marked times (t_1) are the times taken for the first element to swell (Cf. *Figure 3*)

a plot of two profiles for a constant D of 8×10^{-13} m^2 s^{-1}. The sharp front is evident, although not surprisingly there is a steep concentration gradient behind it and a pronounced precursor in front. These latter effects will also cause the front to decelerate with time and thus preclude linear sorption kinetics. It appears therefore that although a straightforward model of deformation control can account for the existence of sharp penetrant fronts, a diffusivity which increases markedly with concentration, albeit without discontinuity, is a necessary additional criterion for pure Case II behaviour in which sorption kinetics are linear.

THE EFFECT OF CHANGING THE EXPONENTIAL FACTOR M

Figure 9 shows the effect on the calculated profiles of changing M, the factor which controls the 'steepness' of the exponential dependence of viscosity on methanol content of the PMMA. The arguments detailed above indicate that M is unlikely to be less than 10 or more than 20. As M is decreased the profiles become more closely spaced, indicating that the sorption rate is dropping off; also the concentration in the precursor increases. When $M = 5$ the front is no longer sharp. It is in fact hardly recognizable and nothing like what is observed. *Figure 10* is a corresponding series of total sorption plots. The effect of M on rate is again apparent, but also the induction time increases with decreasing M. Especially for $M = 5$ but also in general, the induction period appears as an interval in which the sorption rate is slowly increasing rather than remaining at zero. It is also closely correlated with the time taken for the first element to swell to equilibrium as calculated for *Figure 3* and this time is marked on the plots of *Figure 10* as t_1.

EFFECT OF DIFFERENT VALUES FOR DIFFUSIVITY, D, AND VISCOSITY, η_0

(As diffusivity is a measure of rate and viscosity a measure of reciprocal rate, discussion of the effects of these two parameters is made clearer if viscosity is referred to as its reciprocal which we call viscous flow rate ($1/\eta_0$).)

The initial choice of what appeared sensible values for D and $1/\eta_0$, has given a calculated set of transport kinetics very much in line with what is observed experimentally. It is known that the activation energy of diffusion is around 10 kcal mol^{-1}, whereas that for the propagation of Case II fronts in the system PMMA–methanol is more like 25 kcal mol^{-1}.[8] Hence a change in temperature should be expected to affect the diffusion profiles in a more profound way than a simple time scaling. *Figures 11a* and *11b* show a selection of calculated profiles for different values of D and $1/\eta_0$. The central plots use the same values as in *Figures 5a* and *5b*, whereas the plots in the four corners represent the effect of positive or negative changes of around 1/3 of an order of magnitude in the values of D and $1/\eta_0$. The positioning of the plots indicates the values of these parameters on a log co-ordinate system.

Taking the bottom-left to top-right diagonal first where D and $1/\eta_0$ are changed by equivalent amounts in the same sense, it is apparent that the effect is simply one of scaling in time. The corresponding total sorption plots of *Figure 11b* again demonstrate simple time scaling.

Look now at top-left to bottom-right diagonals where a positive change in D is accompanied by a similar but negative change in $1/\eta_0$. It is apparent that the time scale of the process remains roughly constant. There is however a more distinct induction time for the lower right example in *Figure 11b*, which is difficult to detect at all in the top-left plot. The profiles (back to *Figure 11a*) of the top-left plot, where the diffusion rate is lower but the viscous flow rate higher, show some signs of slowing down as they approach each other, and there is a well developed diffusional gradient behind the fronts. Both these contribute to the corresponding curved sorption plot in *Figure 11b*.

The effect of larger changes in D and $1/\eta_0$ in the opposite sense (i.e. along the top-left to bottom-right diagonal of *Figure 11*) are shown in *Figures 12a* and *12b*, where the range covers two decades of rate. It is interesting to compare the profiles in the top figure (*Figure 12a*) with those obtained experimentally for diffusion of methanol in PMMA at 52°C which are reproduced in *Figure 13*[27].

In the bottom diagrams where the viscous flow rate is very much less than the diffusivity, not only is the induction time very apparent but also there is an indication of acceleration of the fronts just before they meet. This is the direct result of the overlapping precursors and has been observed experimentally in polystyrene–alkane systems[9].

The calculated results in *Figures 11* and *12* lead to two interim conclusions. Firstly that the induction time is real and is affected by $1/\eta_0$ but not by D. Secondly that both $1/\eta_0$ and D influence the rate of front traverse even where the diffusion gradient behind the front is too small to be apparent.

THE INDUCTION TIME

Induction times have been measured experimentally for Case II transport in the range 0°–42°C[27] by extrapolation of the linear (or near linear) portion of the sorption curve to the time axis, and these values are listed in *Table 1* and displayed on an Arrhenius plot in *Figure 14*.

The apparent activation energy is 28.3 kcal mol^{-1}. It compares well with the value of 27.0 kcal mol^{-1} obtained from measurements of the influence of temperature on front velocity at constant penetrant concentration[13] and is reasonable for that for viscous creep in a glassy polymer. It follows therefore that measurement of an induction time can give a straightforward indication of the viscosity, or creep behaviour, of a glassy polymer. However it should be emphasized that any such calculation depends on the exact value chosen for M, the measured value of k, the temperature and the molar volume of penetrant. The calculated induction time for 24°C is 4.5 h (measured from *Figure 5b*) and this point is also plotted on *Figure 14*.

THE DEPENDENCE OF TRANSPORT PARAMETERS ON DIFFUSIVITY AND VISCOSITY AND THEIR RELATIONSHIP TO TEMPERATURE

In the subsection before last we explored the effect of relatively small changes in the diffusivity D and viscous flow rate $1/\eta_0$ on the penetrant profiles and total sorption plots. Instead of reproducing a large number of plots to cover a greater range of these parameters we have plotted in *Figure 15* two characteristic parameters as contours on log $1/\eta_0$–log D co-ordinates. They are the induction time, t_{ind}, and the total time taken for the sharp front to traverse from the surface to the central plane of a 1 mm thick sheet

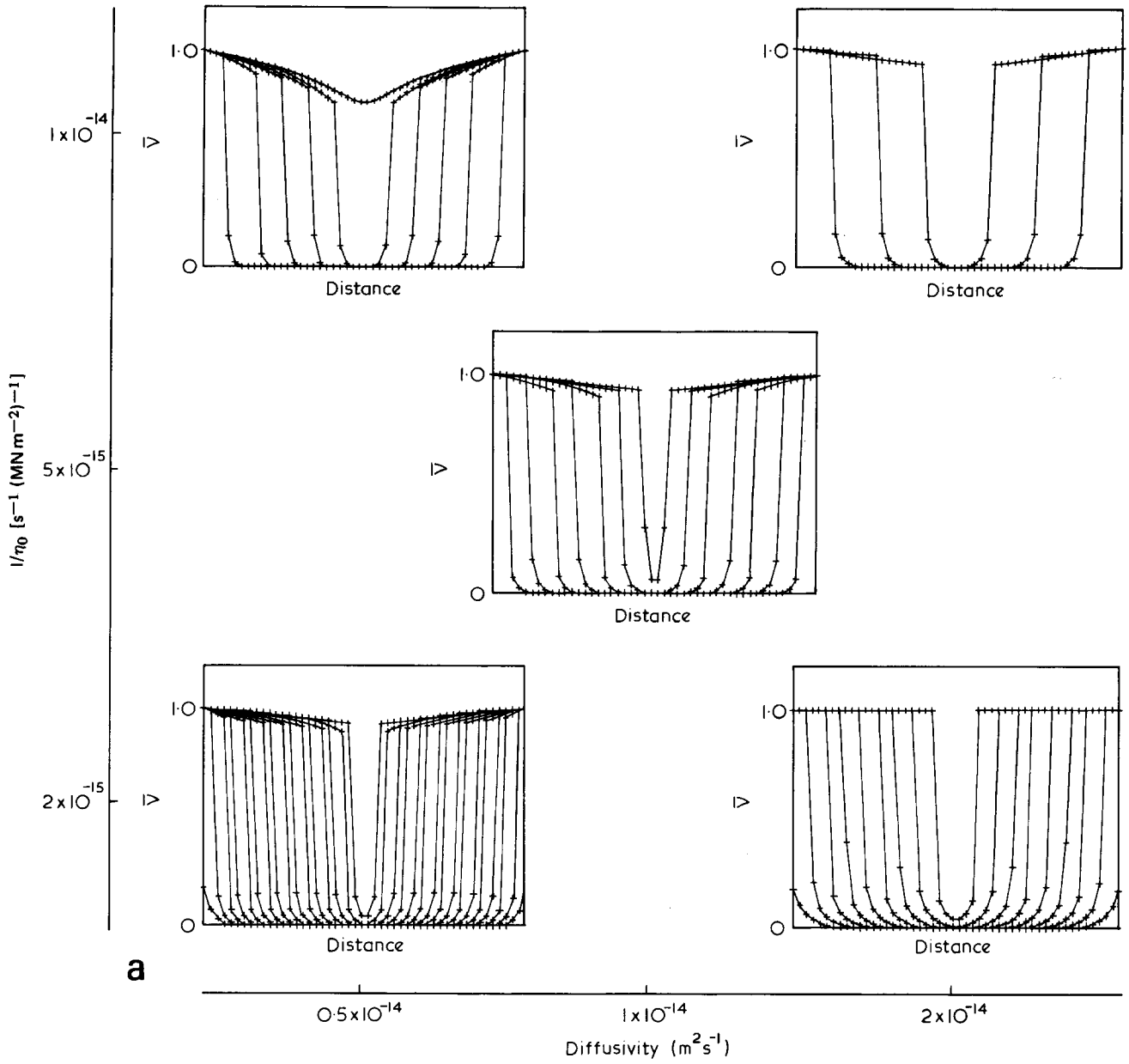

Figure 11a Calculated profile plots showing the effect of changing the diffusivity, and the viscous flow rate, $1/\eta_0$. The profiles are at 10 h intervals. The central plot is again as *Figure 5a* while the surrounding four correspond to positive or negative changes in the diffusivity, D, and the viscous flow rate $1/\eta_0$ of about one third of an order of magnitude

specimen, t_{tr}. For pure Case II behaviour t_{tr} will be less than the total time to equilibrium absorption by an amount equal to t_{ind}. Under conditions where D is smaller and $1/\eta_0$ larger and significant concentration gradients have built up behind the fronts, then $(t_{tr}+t_{ind})$ is less than the total absorption time which is only reached when the concentration gradients behind the fronts (which have reached the central plane) have 'filled in'.

The horizontal (broken) contours on *Figure 15* represent the calculated induction time, t_{ind}, in hours. They demonstrate that this parameter (for the element model) depends only on $1/\eta_0$ and not on D. The calculated contours for t_{tr} are particularly revealing, for it appears that in the centre of the plot and towards the lower right, the front traverse time depends *equally* on viscous flow rate $(1/\eta_0)$ and diffusivity (D). This region of the viscous flow rate–diffusivity domain corresponds to pure Case II transport behaviour with linear kinetics. There is however a boundary towards the top-left marking the stage at which the contours turn towards the vertical. Once established as vertical we are in a regime where the rates depend only on D, the rate $1/\eta_0$ apparently being too large to exert any rate controlling influence on the transport process. In this region the transport behaviour becomes more or less Fickian with $t^{1/2}$ kinetics as the concentration gradients behind the fronts assume a dominant role.

We have measured experimentally values of t_{ind} and t_{tr} over the temperature range 0°–42°C for PMMA–methanol. These data together with the experimental values of k are listed in *Table 1*. Where the sheets were slightly thicker than 1 mm the values of t_{tr} have been corrected accordingly.

Before the experimental values of t_{ind} and t_{tr} are plotted, however, the fact that *Figure 15* is based on calculations in which k is 0.23 and $T=297$K should strictly be taken into account. In effect the position of the experimental points on the vertical scale has been modified by the factor $(k/T)(297/0.23)$ before plotting, but as this factor varies only from 0.9 to 1.2 it has not been incorporated, the

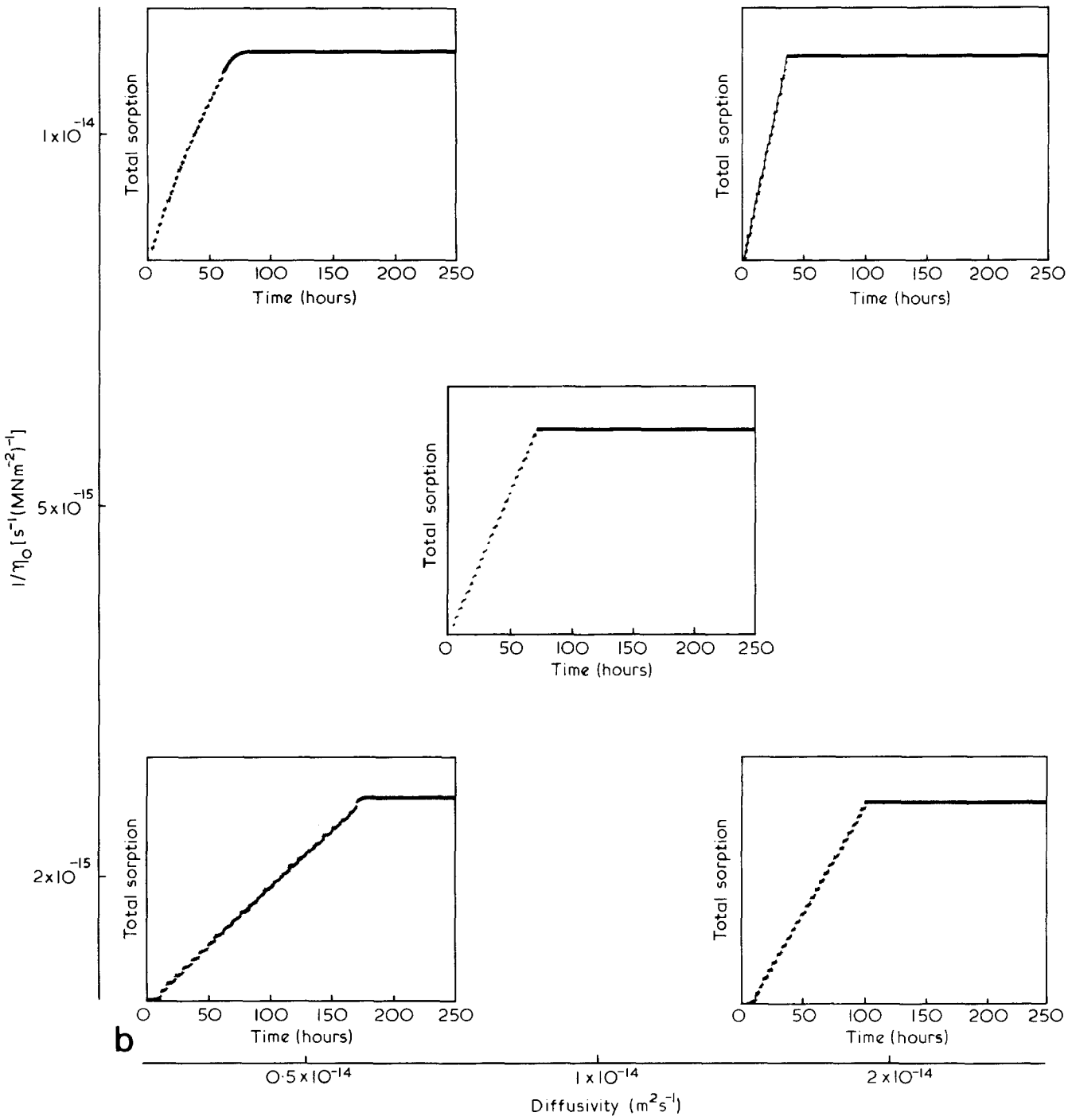

Figure 11b As for *Figure 11a* but showing sorption plots

uncertainties in the experimental values and questions as to the variations of M with temperature being dominant. The experimental data, as values of t_{ind} and t_{tr} at different temperatures, are plottable on *Figure 15* with reference to the two sets of intersecting contours. However, for the sake of clarity they are instead plotted in *Figure 16* on a simplified version of *Figure 15* from which the contours have been omitted. The slope of the experimental line indicates that the viscosity changes about twice as rapidly with temperature as does the diffusivity, which taking the value of 28.3 kcal mol^{-1} for the activation energy for the viscosity controlled process would indicate a value of around 14 kcal mol^{-1} for the activation energy for diffusivity. It has thus proved possible, on the basis of this model, to relate two readily measureable experimental quantities, t_{ind} and t_{tr}, which characterize the Case II process, to the fundamental parameters of diffusivity of the penetrant (D) and the viscous flow rate of the glass ($1/\eta_0$).

CONCLUSIONS

A theory is introduced that accounts for the phenomenon of Case II diffusion which is observed when glassy polymers are swollen in organic penetrants. The theory explains the process in terms of two basic parameters: the diffusion coefficient D and the flow viscosity of the glassy polymer, η_0. The mathematical development is general in that it can describe the complete range of anomalous behaviour between the Fickian and Case II extremes.

Case II and related diffusion processes have characteristic features which have been well documented

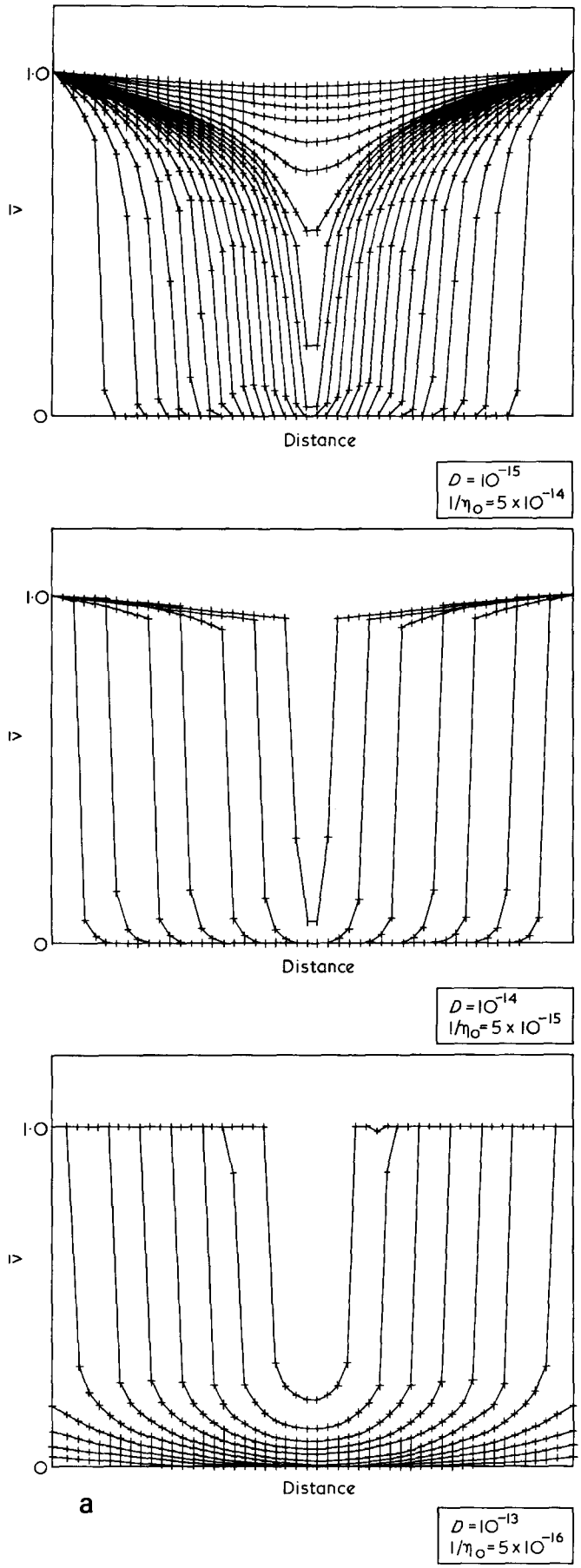

Figure 12a Calculated profile plots corresponding to the top-left — bottom-right diagonal of *Figure 11a*, but showing the effects of changes $\pm D$, $\mp(1/\eta_0)$ of one order of magnitude

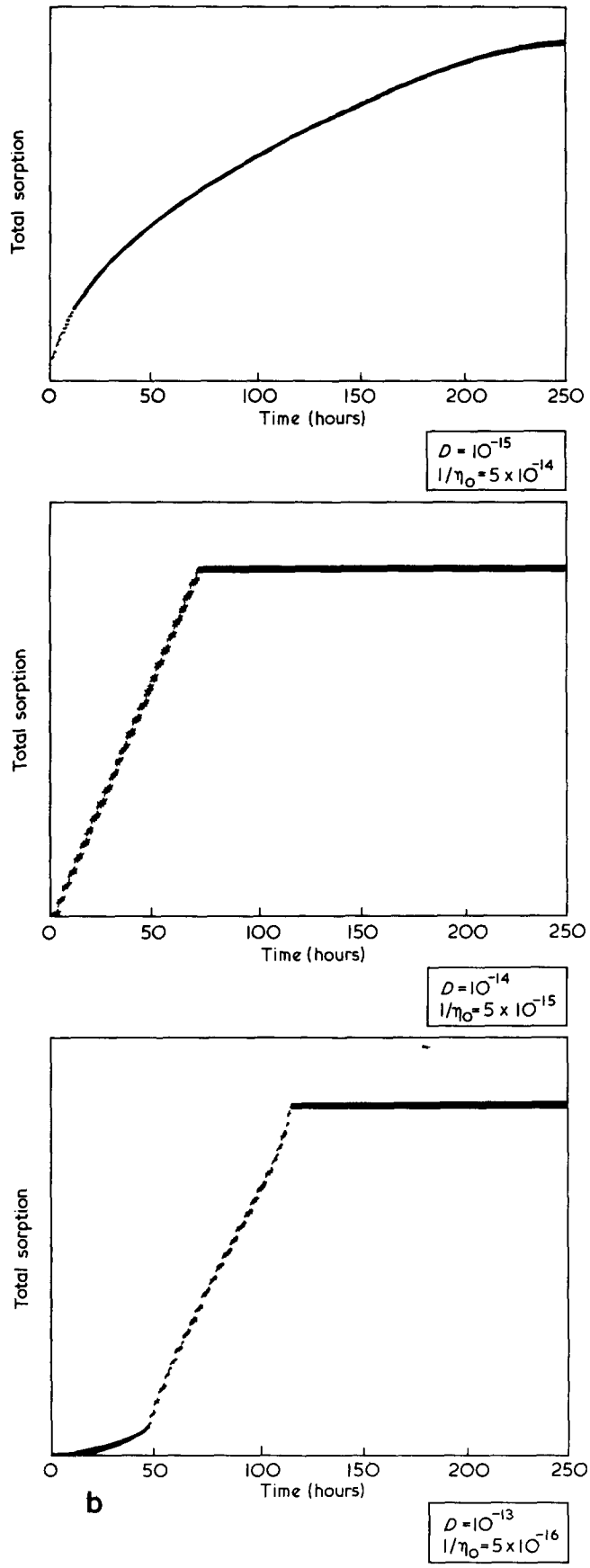

Figure 12b Sorption plots corresponding to *Figure 12a*

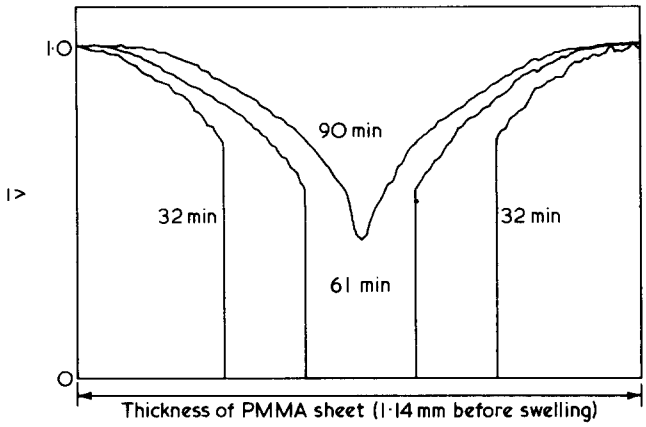

Figure 13 Experimental concentration profiles measured for the system PMMA–methanol at 52°C. The times are marked on the profiles

Table 1 Experimental values of induction time, front traverse time and k for PMMA–methanol 1 mm sheets at the temperatures indicated

Temperature (°C)	t_{ind} (h)	t_{tr} (h)	k
0	192	3600	0.20
10	38	654	0.20
15	16	333	0.20
24	2.5	70	0.23
42	0.08	60	0.29

in the literature over a number of years. Of these the existence of a sharp penetrant front and its linear propagation with time are central to the Case II process itself, as are the associated linear sorption kinetics. In addition there have been observations of an induction period at the start of the process, and an acceleration in front traverse rate at the end, the latter phenomenon having previously been termed Super Case II[9]. It has also been established that an increase in viscous flow rate which is not matched by a corresponding increase in diffusivity, results in a more prominent concentration gradient behind the fronts, which in the extreme leads to the re-establishment of Fickian kinetics. Such behaviour is often associated with absorption at higher temperatures. The theory predicts this complete spectrum of behaviour in terms of simple physical principles.

The specific conclusions of the work can be summarized as follows:

(1) The theory predicts that a surface element of polymer glass which is thin enough so that diffusional resistance can be neglected, will initially imbibe penetrant at a very slow rate, but that this rate will increase sharply in an autocatalytic manner at longer times.

(2) Calculations, over time increments, which alternately determine changes to the concentration profile at constant activity and changes to the activity profile at constant concentration/activity ratio, effectively model the diffusion process. When realistic values for the diffusivity of methanol in PMMA, the creep rate of PMMA and its variation with penetrant concentration are used, Case II type behaviour is predicted.

(3) The calculated diffusion process for PMMA–methanol at room temperature has the following features:

(i) Sharp concentration fronts to within the resolution of the finite element calculation.
(ii) Small concentration gradient behind the fronts.
(iii) Constant front penetration velocity.
(iv) Linear sorption kinetics as a consequence of (ii) and (iii).

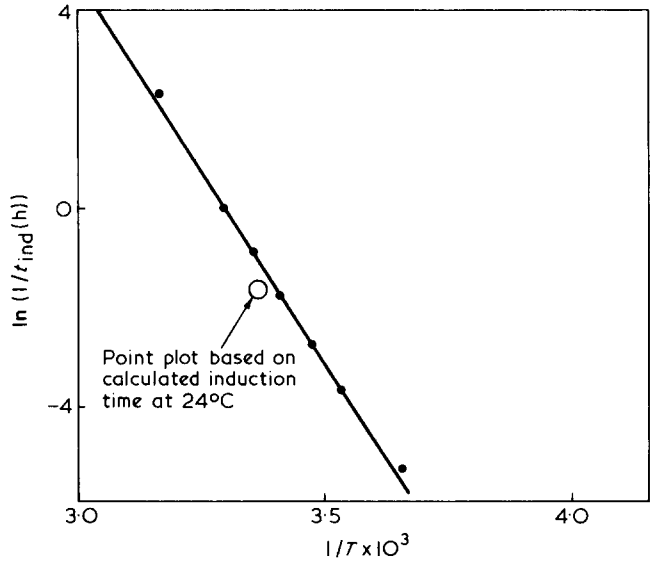

Figure 14 Graph of ln $(1/t_{ind})$ vs. $1/T$, where the induction times have been determined experimentally. Also plotted is the calculated induction time for the specimen at 24°C

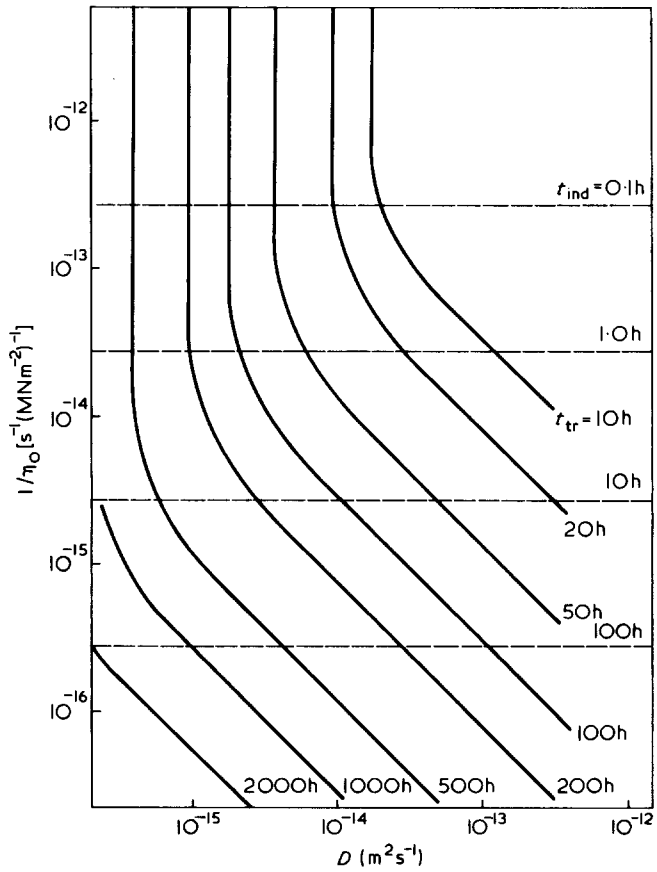

Figure 15 Two sets of contours representing the calculated values of the parameters t_{ind} (broken lines) and t_{tr} (solid lines) plotted with log diffusivity, D, and log viscous flow-rate $(1/\eta_0)$ as co-ordinates

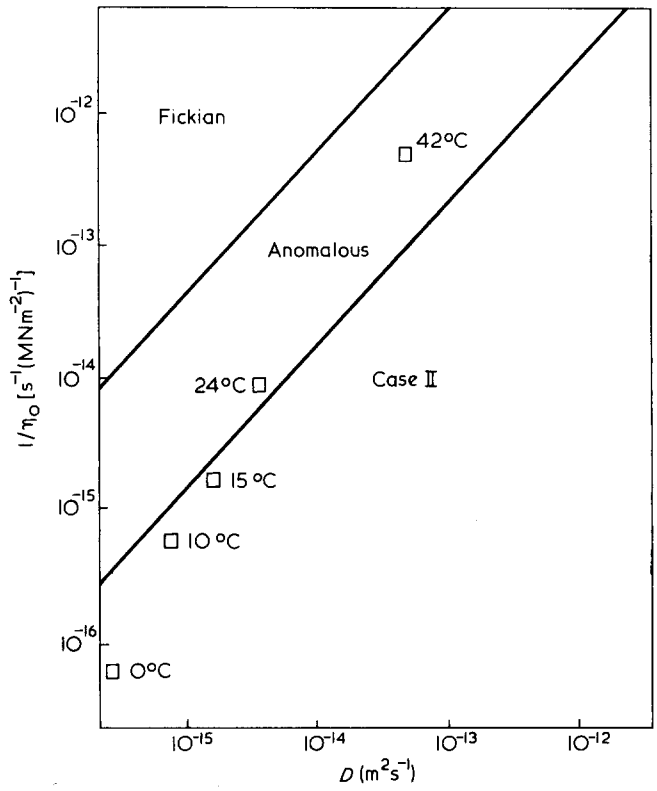

Figure 16 A schematic representation of *Figure 15* showing three regions: Case II diffusing with linear kinetics where the t_{tr} contours are at 45°; Fickian ($t^{1/2}$) where the t_{tr} contours are vertical; and a transition region of anomalous diffusion. Superimposed on this diagram are experimental data pairs of t_{ind} and t_{tr} plotted by reference to the appropriate contours (*Figure 15*). The experimental plots are annotated with the temperature at which they are measured, and their co-ordinates give the values of D and $1/\eta_0$ which, on the basis of this theory, would account for the observed behaviour

(v) A small precursor ahead of the front.

(vi) An induction period before front penetration begins, which is an inherent feature of the process.

With the exception of the small precursor all of these predicted features are acknowledged as experimental features of the Case II process.

(4) The calculated Case II process has characteristic time constants, such as the induction time and time for fronts to meet in a 1 mm specimen, which are in remarkable agreement with experimental values. It is concluded that the closeness of quantitative agreement, to within better than 20%, must be to some extent fortuitous because of the uncertainties in the estimation of diffusivity, viscous flow (creep) rate and the way in which these parameters vary with penetrant concentration.

(5) Reduction of the diffusivity parameter in relation to the viscous flow rate leads to an increase in the diffusion gradient behind the fronts. This destroys the linear quality of the kinetics which tend towards square root dependence on time. This behaviour corresponds to that observed in the system PMMA–methanol at temperatures above 40°C, this correspondence being a consequence of the fact that the activation energy for viscous flow is greater than that for diffusion.

(6) The induction time depends linearly on the reciprocal of the viscous flow rate (i.e. it is proportional to the viscosity, η_0). It is independent of diffusivity (D).

(7) The constant rate at which the front traverses the specimen in the Case II process depends equally and linearly on both the log of the viscous flow rate ($1/\eta_0$) and the log of the diffusivity (D).

(8) Comparison between the predicted and measured values of induction time, t_{ind}, and front traverse time, t_{tr}, indicates that for PMMA–methanol, the activation energy for diffusion is 14 kcal mol^{-1} and the activation energy for viscous flow is twice this value at 28.3 kcal mol^{-1}.

(9) In situations where the viscous flow rate is very much less than the diffusivity, the induction period is a marked feature of the calculated sorption curve. Additionally, under these conditions there is a distinct acceleration in sorption rate just before the fronts meet.

ACKNOWLEDGEMENTS

The authors wish to thank Professor H. B. Hopfenberg for his encouragement of this work and for stimulating discussion both in Cambridge and Raleigh. They are also grateful to Dr C. Cohen for helpful suggestions regarding the applicability of equation (12), to Professors J. H. Petropoulos and A. Peterlin for criticism and encouragement, to Mr R. P. Collins and Mr G. R. Mitchell for assistance with the finite element calculations, and to Professor R. W. K. Honeycombe for the provision of laboratory facilities. The work was funded under SRC grant No. (GR/A/68141) and the authors are grateful for this too.

REFERENCES

1 Alfrey, T., Gurnee, E. F. and Lloyd, W. G. *J. Polym. Sci. (C)* 1966, **12**, 249
2 Frisch, H. L., Wang, T. T. and Kwei, T. K. *J. Polym. Sci. (A2)* 1969, **7**, 879
3 Petropoulos, J. H. and Roussis, P. P. *J. Memb. Sci.* 1978, **3**, 343
4 Peterlin, A. *J. Polym. Sci. (B)* 1965, **3**, 1083
5 Peterlin, A. *Makromol. Chem.* 1969, **124**, 136
6 Peterlin, A. *J. Res. Nat. Bur. Std.* 1977, **81A**, 243
7 Peterlin, A. *J. Polym. Sci., Polym. Phys. Edn.* 1979, **17**, 1741
8 Thomas, N. L. and Windle, A. H. *Polymer* 1978, **19**, 255
9 Jacques, C. H. M., Hopfenberg, H. B. and Stannet, V. 'Permeability of Plastic Films and Coatings', (Ed. H. B. Hopfenberg), Plenum, New York (1974), p. 73
10 Astarita, G. and Sarti, G. C. *Polym. Eng. Sci.* 1978, **18**, 388
11 Sarti, G. C. *Polymer* 1979, **20**, 827
12 Thomas, N. L. and Windle, A. H. *Polymer* 1977, **18**, 1195
13 Thomas, N. L. and Windle, A. H. *Polymer* 1980, **21**, 613
14 Smith, K. J. Theories of Chain Coiling, Elasticity and Viscoelasticity, from 'Polymer Science', (Ed. A. D. Jenkins), Vol 1, North Holland, (1973)
15 Flory, P. J. 'Principles of Polymer Chemistry', Cornell University Press, Ithaca (1953), Ch. 12
16 Crank, J. *J. Polym. Sci.* 1953, **11**, 151
17 Thomas, N. L. and Windle, A. H. *Polymer* 1981, **22**, 627
18 Turner, S. 'Physics of Glassy Polymers', (Ed. R. Haward), Applied Science Publishers, London (1973), p. 252
19 Ogorkiewicz, R. M. 'Engineering Properties of Thermoplastics', Wiley, London (1970)
20 Gibbs, J. W. 'Collected Works', Yale University Press, 1948
21 Park, G. S. 'Treatise on Coatings', (Ed. R. R. Myers, and J. S. Long), Dekker, N.Y. (1976), Vol. 2, Part II, Ch. 9
22 Wang, T. T. and Kwei, T. K. *Macromolecules* 1973, **6**, 919
23 Hopfenberg, H. B., Nicholais, L. and Drioli, E. *Polymer* 1976, **17**, 195
24 Thomas, N. L. and Windle, A. H. *J. Memb. Sci.* 1978, **3**, 337
25 Weinberg, D. *J. Memb. Sci.* 1978, **3**, 309
26 Crank, J. *Trans. Faraday Soc.* 1951, **47**, 450
27 Thomas, N. L. *Ph.D. Thesis*, Cambridge University, 1978